Nuclear Inst. and Methods in Physics Research, A 875 (2017) 27–34

Contents lists available at ScienceDirect

Nuclear Inst. and Methods in Physics Research, A

journal homepage: www.elsevier.com/locate/nima

Study of gain homogeneity and radiation effects of Low Gain Avalanche Pad Detectors

C. Gallrapp [a,*], M. Fernández García [b], S. Hidalgo [c], I. Mateu [a,d], M. Moll [a], S. Otero Ugobono [a], G. Pellegrini [c]

[a] CERN—European Organization for Nuclear Research, Geneva, Switzerland
[b] IFCA—Instituto de Física de Cantabria (CSIC-UC), Santander, Spain
[c] Centro Nacional de Microelectrónica, IMB-CNM-CSIC, Barcelona, Spain
[d] CIEMAT—Centro de Investigaciones Energéticas, Medioambientales y Tecnológicas, Madrid, Spain

ARTICLE INFO

Keywords:
Silicon detectors
Low gain APD
LGAD
Charge multiplication
Radiation damage

ABSTRACT

Silicon detectors with intrinsic charge amplification implementing a n^{++}-p^{+}-p structure are considered as a sensor technology for future tracking and timing applications in high energy physics experiments. The performance of the intrinsic gain in Low Gain Avalanche Detectors (LGAD) after irradiation is crucial for the characterization of radiation hardness and timing properties in this technology. LGAD devices irradiated with reactor neutrons or 800 MeV protons reaching fluences of 2.3×10^{16} n_{eq}/cm^2 were characterized using Transient Current Technique (TCT) measurements with red and infra-red laser pulses. Leakage current variations observed in different production lots and within wafers were investigated using Thermally Stimulated Current (TSC). Results showed that the intrinsic charge amplification is reduced with increasing fluence up to 10^{15} n_{eq}/cm^2 which is related to an effective acceptor removal. Further relevant issues were charge collection homogeneity across the detector surface and leakage current performance before and after irradiation.

1. Introduction

The ongoing preparation for the luminosity upgrade of the Large Hadron Collider (LHC) at CERN is imposing new requirements on all detector systems used in HL-LHC particle physics experiments. Especially the increased radiation hardness of the tracking detectors towards fluences up to 2×10^{16} n_{eq}/cm^2 for pixel and 1.5×10^{15} n_{eq}/cm^2 for strip detectors led to the development of new silicon sensor technologies and designs [1,2]. Some of these upcoming detector concepts are focusing on an increased timing resolution in the order of tens of pico seconds. Further, these new tracking detector concepts need to maintain properties such as radiation hardness and spatial resolution known from existing technologies [3].

One of these proposed technologies are Low Gain Avalanche Detectors (LGAD). For this detector technology the timing properties are expected to improve compared to regular silicon detectors due to an amplified signal caused by an intrinsic charge multiplication [4]. The challenge in this approach is to amplify the signal in a way that the overall signal to noise ratio (SNR) of the device is improving as well. This means for example that the leakage current must be kept at a low level to avoid an increased noise. The position resolution, on the other hand, must not be deteriorated compared to standard silicon detectors. To achieve this aim a homogeneous charge multiplication across the sensor surface is especially important. If this is not reached an analysis of the collected charge in the experiment becomes impossible.

The aim of this work is to characterize the charge collection and the charge multiplication of pad detectors based on the LGAD design after proton and neutron irradiations. Special focus is directed towards the gain performance as it is strongly influenced by irradiation and is expected to represent the main factor for timing properties.

2. LGAD structure and measurement techniques

Low Gain Avalanche Detectors (LGAD) are based on a regular p-type planar sensor design with the add-on of a highly p-doped multiplication layer at the np-junction. This p^{+} implant shapes the electric field in the sensor to reach impact ionization from electrons drifting in the high field region at the junction. The electric field is shaped to peak around 2 to 4×10^{5} V/cm [3,5], but clearly the total gain depends as well on the

* Corresponding author.
E-mail address: christian.gallrapp@cern.ch (C. Gallrapp).

http://dx.doi.org/10.1016/j.nima.2017.07.038
Received 16 November 2016; Received in revised form 22 June 2017; Accepted 19 July 2017
Available online 26 August 2017

shape of the implant. The magnitude of the impact ionization depends on the electric field determined by the doping concentration and profile of the multiplication layer. This makes it possible to tune the intrinsic amplification (gain) of the detectors. The advantage of the introduced gain is an increased signal to noise ratio which is expected to improve timing properties in LGAD devices compared to regular planar sensors. In addition leads an increased signal to an improved signal-to-noise ratio (SNR) in radiation damaged highly segmented sensors where the noise is not dominated by the radiation induced leakage current [6]. Timing properties and performance after irradiation are the reason for increased interest in this technology which led to several activities within the CERN RD50 collaboration [7].

Several lots[1] of LGAD based pad detectors have been fabricated by the Centro Nacional de Microelectrónica (CNM, Barcelona) in p-doped float-zone (FZ) silicon wafers with a resistivity $\rho > 10\,\mathrm{k\Omega\,cm}$ and ⟨100⟩ crystal orientation. Two lots of LGAD sensors, both with boron-doped multiplication layers with implantation doses of $1.6{\times}10^{13}\,\mathrm{cm^{-2}}$, $2.0{\times}10^{13}\,\mathrm{cm^{-2}}$ and $2.2\times10^{13}\,\mathrm{cm^{-2}}$ using an implantation energy of 100 keV, have been produced at CNM corresponding to the lots 6474 and 7062. Regions with high electric field at the border of the multiplication layer can cause an early breakdown in LGAD based devices. A junction termination extension (JTE) was added to the design in order to assure the operation of the detector up to a bias voltage of 1000 V. This n-doped region overlaps with the n^{++} electrode and moderates the peak field at the border of the multiplication layer [5,8,9]. Approaches are undertaken to understand if more homogeneous amplification regions throughout larger sensor areas can be achieved by separating the amplification region from the charge collecting electrodes. This concept is implemented in the so-called iLGAD (inverse-LGAD) concept, where p-strips are implemented on the front side of the device and the amplification region on the back side [10]. A cross-section of an LGAD device is given in Fig. 1 and illustrates the structure of the multiplication layer and the JTE. The figure also shows the electrical circuit and the different laser configurations used during TCT measurements.

2.1. LGAD structure and device description

The discussed LGAD lots include pad structures with a sensitive area of 5 mm×5 mm in a 300 µm thick material. Standard n-in-p structures without multiplication layer produced on an additional wafer are also available as reference. The expected operation voltage can vary between the full depletion voltage and 1000 V. The mask design comprises optical windows in the front and back side metallization for illumination with a light source. Due to the absence of a guard ring structure in the design it is impossible to distinguish surface from bulk current contributions. This point is especially important as it was found that the leakage current in these devices can vary up to three orders of magnitude between samples produced on the same wafer [8,6,11].

Measurements at different temperatures have shown that there is only little current decrease with decreasing temperature. Since bulk current scales exponentially with temperature it was concluded that the observed excess currents in some of the samples were not originating from defects in the bulk, but are rather from surface imperfections or close to surface problems of unknown origin [8]. A radiation damage study performed on these sensors showed an increased positive space charge in devices with high excess current before irradiation as compared to devices with lower current before irradiation [6,11]. This lead to the assumption that the excess current is generated close to the front side, i. e. the $n^{++}p^{+}$-junction side. Since it is generated close to the front side, this additional current flowing through the amplification region and the bulk of the device would correspond to a hole current. This current could be able to compensate the overall space charge towards a more positive space charge by hole trapping [6,11]. Up till now neither of these assumptions about the origin of excess leakage current could finally be confirmed.

[1] Production lot consisting of several wafers using the same mask design. For LGAD devices it is possible that within one lot different multiplication layer doses were used. For traceability reasons each lot is associated with an unique lot number which are also used as reference in this report.

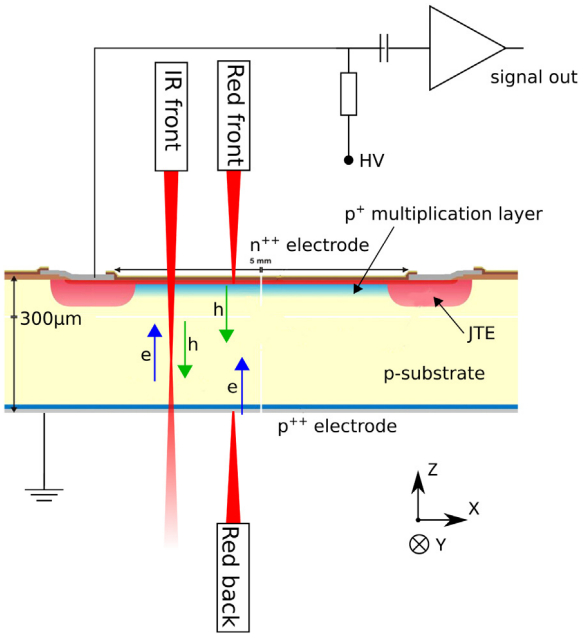

Fig. 1. Cross-section of a LGAD pad structure illustrates the n^{++} and p^{++} doped readout electrodes as well as the multiplication layer. The junction termination extension (JTE) surrounds the entire pn-junction to reduce peaks in the electric field [5]. The design does not include a guard ring structure but provides optical windows for measurements with red and infra-red lasers. The layout of the TCT setup shows the three configurations that were used to perform either hole or electron injection by red laser pulses or to generate a minimum ionizing particle (MIP) like generation of e–h pairs by IR laser pulses.

Table 1
Table of irradiated samples tested in this study indicating the collected fluence for each type of irradiation.

800 MeV protons	Reactor neutrons
$9.87{\times}10^{11}\,n_{eq}/cm^2$	
$1.36{\times}10^{13}\,n_{eq}/cm^2$	$1{\times}10^{13}\,n_{eq}/cm^2$
$1.04{\times}10^{14}\,n_{eq}/cm^2$	$1{\times}10^{14}\,n_{eq}/cm^2$
$9.19{\times}10^{14}\,n_{eq}/cm^2$	$1{\times}10^{15}\,n_{eq}/cm^2$
$2.30{\times}10^{16}\,n_{eq}/cm^2$	$1{\times}10^{16}\,n_{eq}/cm^2$

Studies focusing on the properties of LGAD sensors after irradiation have been performed with samples from lot 6474 [6]. These studies included only samples with leakage currents below few µA at 20 °C before irradiation effectively excluding devices with increased leakage current. For these studies neutron, proton or pion irradiations were performed. Several samples were even irradiated in multiple fluence steps to compare the radiation hardness as a function of fluence [6].

Samples from lot 7062 which are discussed in this paper were irradiated with reactor neutrons at the Jožef Stefan Institute in Ljubljana, Slovenia [12] and with 800 MeV protons at the Los Alamos National Lab in Los Alamos, USA [13,14]. Table 1 summarizes the different samples indicating the type of irradiation and the collected fluence.

2.2. Transient current technique and signal formation

Earlier studies showed a significant gain degradation in LGAD devices for fluences above $1{\times}10^{14}\,n_{eq}/cm^2$ [6]. This behavior was attributed to a reduction of effective doping in the p^{+}-doped multiplication layer [6,11], with smaller electric field at the junction and thus less charge amplification. The Transient Current Technique (TCT) was proposed to probe the depletion depth of the p^{+}-layer as a function of

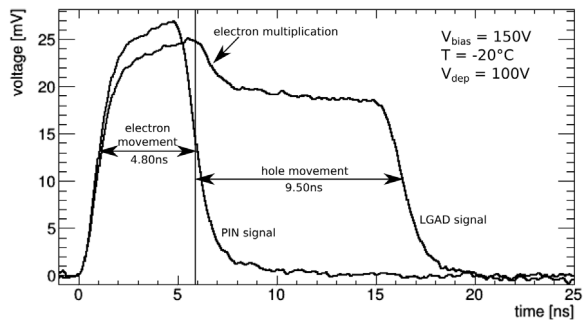

(a) Electron injection [6].

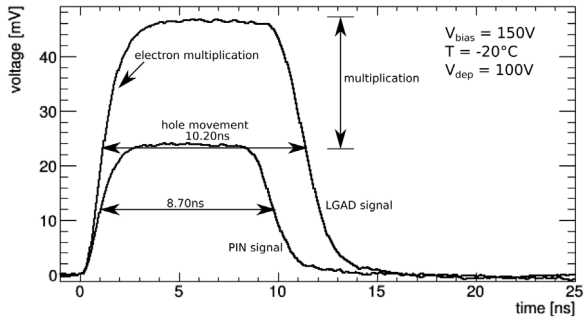

(b) Hole injection.

Fig. 2. The two laser configurations; hole and electron injection generated by red laser pulses are shown in Fig. 2(a) and (b) respectively. For both cases a LGAD signal is shown with an unscaled signal of a PIN diode to illustrate the difference in the signal formation and amplification. It needs to be pointed out that the increased drift time in the LGAD device versus the PIN diode at the same voltage is arising from the fact that part of the voltage in the LGAD is dropping over the gain layer. The bulk of the LGAD has thus a lower electric field in the bulk and consequently a longer charge drift time.

voltage. Here, red light (λ = 660 nm) pulses with a short absorption length (~3 μm in silicon [15,16]) are injected in the junction side of the device to measure the signal induced by the hole current. This signal is only visible after full depletion of the p^+-layer. Measurements on LGAD samples with leakage current in the range of few μA showed that the voltage needed to deplete the multiplication layer after irradiation decreases. This effect was associated with an acceptor removal due to the removal of boron in the multiplication layer [6,11] which would also explain the observed gain degradation. An alternative explanation for the gain degradation in LGAD devices is based on the simulation of LGAD structures which showed that the effect could be caused by charge trapping in the device [17].

The Transient Current Technique further allows to draw conclusions about the shape of the electric field inside a sensor and about its charge collection properties [18]. In this study red (660 nm) and infra-red (1064 nm) picosecond laser pulses were used to generate charge carriers in the sensor. The layout of the TCT setup in Fig. 1 shows the different laser configurations used in this study. Illumination with infra-red pulses provides the possibility to simulate the sensor response to minimum ionizing particles by forming a path of electron hole pairs crossing the device. Red laser pulses injected on the front and back side on the other hand allow to study the behavior of electrons and holes individually.

Electron injection (Red laser on back electrode) allows to characterize the movement of electrons traversing the silicon bulk until they reach the multiplication layer. Once the electrons reach the junction the high peak field causes impact ionization and generates additional electron hole pairs. While all the electrons are collected, the holes start to move towards the back side of the sensor. The corresponding waveform shown in Fig. 2(a) indicates the different signal contributions as a function of time. The waveform of a PIN diode also shown in the plot can be used to determine the gain of the LGAD device.

Hole injection (Red laser on front electrode) on the other hand shows the movement of holes related to two generation mechanisms. There are holes generated directly by the laser pulse but also holes generated by impact ionization of the electrons which were generated by the laser pulse. The fact that holes are created by two mechanisms in the same time scale makes it impossible to determine the individual signal contributions. A lower gain factor compared to electron injection is expected for hole injection as part of the charge carriers are created too close to the front electrode to travel through the full amplification layer thus could not contribute to the signal amplification. The waveform in Fig. 2(b) illustrates the pulse shape variation for hole injection between a LGAD and a PIN device. Here, the area difference between the two waveforms can be interpreted as the contribution due to the amplification in the LGAD device. This is only possible since the PIN diode design corresponds to the LGAD design without the amplification layer. Also, a monitoring system for the light intensity is part of the TCT setup and was used to assure that all diodes were illuminated with the same power. Care was taken to understand the reproducibility of the laser measurements. The laser stability was measured with a commercial reference diode over a time period of 5 months. During this time a laser stability better than 3 % was confirmed. A set of 5 sensors was measured twice in the setup with a complete dismounting of the sample boards from the setup in between the measurements. The reproducibility of the obtained CCE data for the identical sensors was better than 2 % for the full voltage range. Finally, a study on 5 diodes irradiated up to a fluence of $9\times10^{14}\,n_{eq}/cm^2$ comparing beta source measurements to laser measurements was performed on the laser setup used in this work, giving an agreement of better than 6 % over the full voltage range up to 1000 V [19].

While the typical procedure of a TCT measurement consists of a voltage scan at a fixed position it is also possible to perform scans in the XY plane (see axis in Fig. 1) to investigate the homogeneity of a device. The objective of the homogeneity measurements is to investigate variations in the charge collection and the gain across the surface. Voltage scans on the other hand are used to understand the growth of the gain depending on the applied bias voltage. Multiple voltage scans at varying positions allow to probe the homogeneity locally and to study the dependence on the bias voltage. The sample temperature was fixed to −20 °C for all measurements in order to exclude signal variations related to temperature fluctuations and to limit the current for highly irradiated samples. To keep the scan time at a reasonable level a step width of 120 μm was used to scan the entire surface of 5 mm×5 mm in the hole injection configuration. For electron injection and infra-red measurements a step width of 25 μm was selected to scan an area of 1 mm×1 mm.

3. Characterization

The characterization of LGAD devices from lot 7062 consists of current and capacitance measurements as a function of voltage (IV and CV) as well as TCT measurements using hole injection, electron injection and IR laser pulses. Measurements before and after irradiation were performed to understand radiation effects on the devices. The same measurements have been performed on an unirradiated reference PIN diode to calculate the intrinsic gain of the LGAD devices. Here, the gain is defined as the ratio of the collected charge in a LGAD device to the collected charge of the undamaged reference sensor without amplification layer.

3.1. Characterization before irradiation

A set of three LGAD devices (lot 7062) was available for investigations before irradiation. Similar to measurements mentioned earlier [6,11], the samples in Fig. 3(a) exhibited a high leakage current.

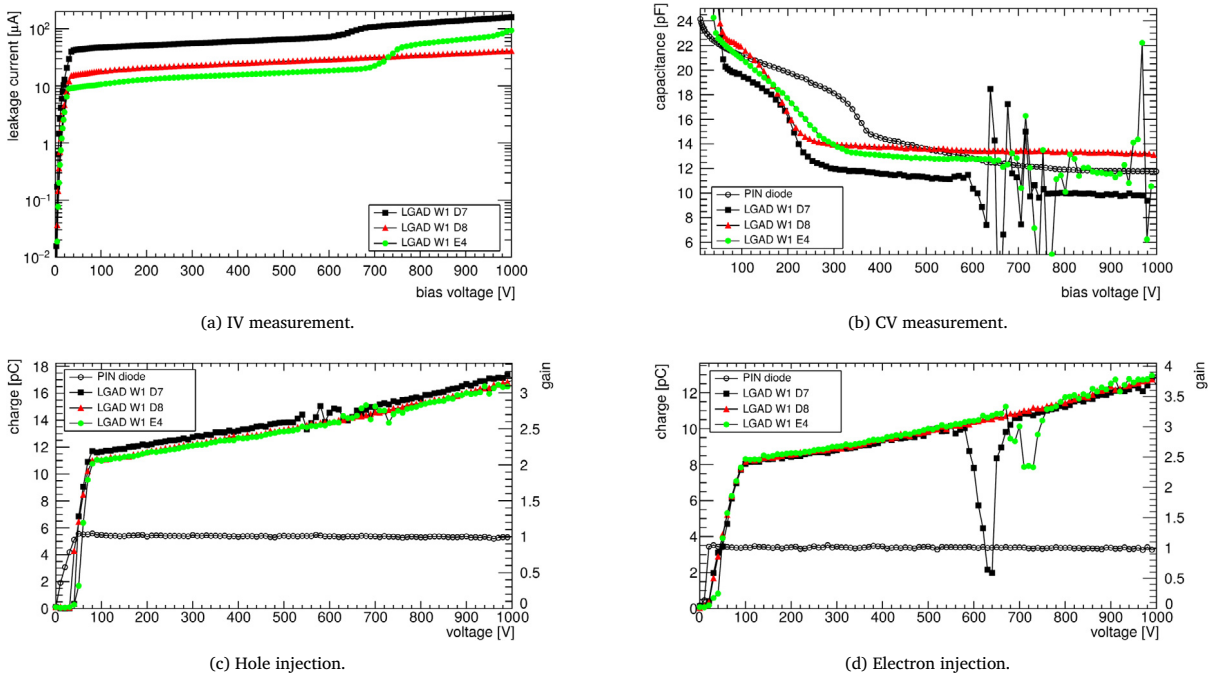

(a) IV measurement.

(b) CV measurement.

(c) Hole injection.

(d) Electron injection.

Fig. 3. Current (a) and capacitance (b) as a function of the applied bias voltage for unirradiated LGAD devices. Charge collection in unirradiated samples for hole injection (c) and electron injection (d). Charge loss at certain voltages corresponds to current and capacitance variations in IV and CV measurements. The measurement results with a gain of 1 correspond to the reference diode. The mean charge for voltages ≥ 500 V was used as the reference to calculate the gain of the LGAD devices. Measurements correspond to lot 7062.

Contrary to other measurements unexpected current steps in two of the samples appeared at about 700 V. Capacitance measurements in Fig. 3(b) revealed bias voltage ranges with high noise coinciding with the current steps in the IV measurement.

TCT measurements with hole and electron injection shown in Fig. 3(c) and in Fig. 3(d) show the charge collection increase with bias voltage. The mean collected charge of the PIN diode for bias voltage values above 500 V was used as the reference charge to calculate the gain in the LGAD devices. Measurements with electron injection in Fig. 3(d) show a gain increase up to 3.8 for a bias voltage of 1000 V. As expected, the gain for hole injection in Fig. 3(c) is below the one for electron injection. This behavior is related to the fact that not all electrons created during hole injection contribute to charge multiplication. The charge measurement for hole and electron injection also show regions with increased noise corresponding to the voltage range coinciding with the current steps observed in the IV measurement. High frequency current fluctuations in the voltage range make it impossible to determine a stable baseline offset which smears the TCT signal and with it the calculated charge. As a result it was not possible to separate the collected charge from the noise causing a noticeable charge decrease in the voltage range of the current steps observed in IV measurements.

3.2. Characterization after neutron and proton irradiation

Charge collection measurements with TCT using hole and electron injection as well as IR pulses were performed on neutron and proton irradiated LGAD structures. Results as a function of the applied bias voltage are shown in Fig. 4. For each sample a set of four measurements was performed at different positions within the optical window of the device in order to investigate charge and gain variations across the sensor surface. The four positions where selected based on an initial surface scan to identify homogeneity variations. These measurement positions were placed at a distance of more than 500 µm between each other to avoid interferences due to the laser spot size of about 10 µm.

The collected charge measured as a function of the bias voltage decreases with fluence. Up to fluences of 1×10^{14} n_{eq}/cm^2 the charge collection in LGAD devices exceeds an unirradiated PIN diode. For higher fluences no contribution to the collected charge due to amplification can be observed. Further a good agreement in the charge collection degradation between proton and neutron irradiation for hole and electron injection and IR pulses is visible. This becomes even more visible by looking at the charge collection as a function of fluence in Fig. 5 for bias voltage values of 1000 V. Still, similar gain behavior for IR pulses and electron injection can be observed. The gain observed during hole injection in irradiated samples is, as before irradiation, lower than the gain for measurements using electron injection or IR pulses.

Earlier studies on devices corresponding to lot 6474 and lot 7062 with low leakage current showed a shift of the onset of the amplification to lower bias voltages [6]. The investigated samples with high leakage current corresponding to lot 7062 show the opposite behavior. Here the onset of the amplification shifts to higher bias voltages. This becomes especially visible for the measurements performed at fluences of about 1×10^{14} n_{eq}/cm^2 where the onset of the amplification shifts noticeably compared to lower fluences. In addition a strong variation between the individual measurement positions is also visible. In case of the proton irradiated samples, a measurement at one position at 1×10^{14} n_{eq}/cm^2 does not show any amplification at all up to 1000 V. Also noticeable are the charge collection and gain variations between the IR pulse measurements performed on four different positions of the devices with a fluence of 1.36×10^{13} n_{eq}/cm^2 for proton and 1×10^{14} n_{eq}/cm^2 for neutron irradiation. For both devices the charge collection between the four different measurement positions varies in the bias voltage range from the amplification onset up to 1000 V. The delayed onset of the amplification as well as the charge collection and gain variation depending on the measurement position on the sample have not been observed before [6,11].

In order to assure that the measurement system did not cause any abnormalities a review of its performance was performed. This review included a comparison of the injected charge of the laser pulses as well as the temperature during the measurement. No abnormal behavior was found in the review which would explain the observed behavior during the measurement of the device.

Similar to the explanation for the abnormal leakage current in unirradiated LGAD devices the observed behavior might be explained with a contamination of the silicon lattice of the affected devices.

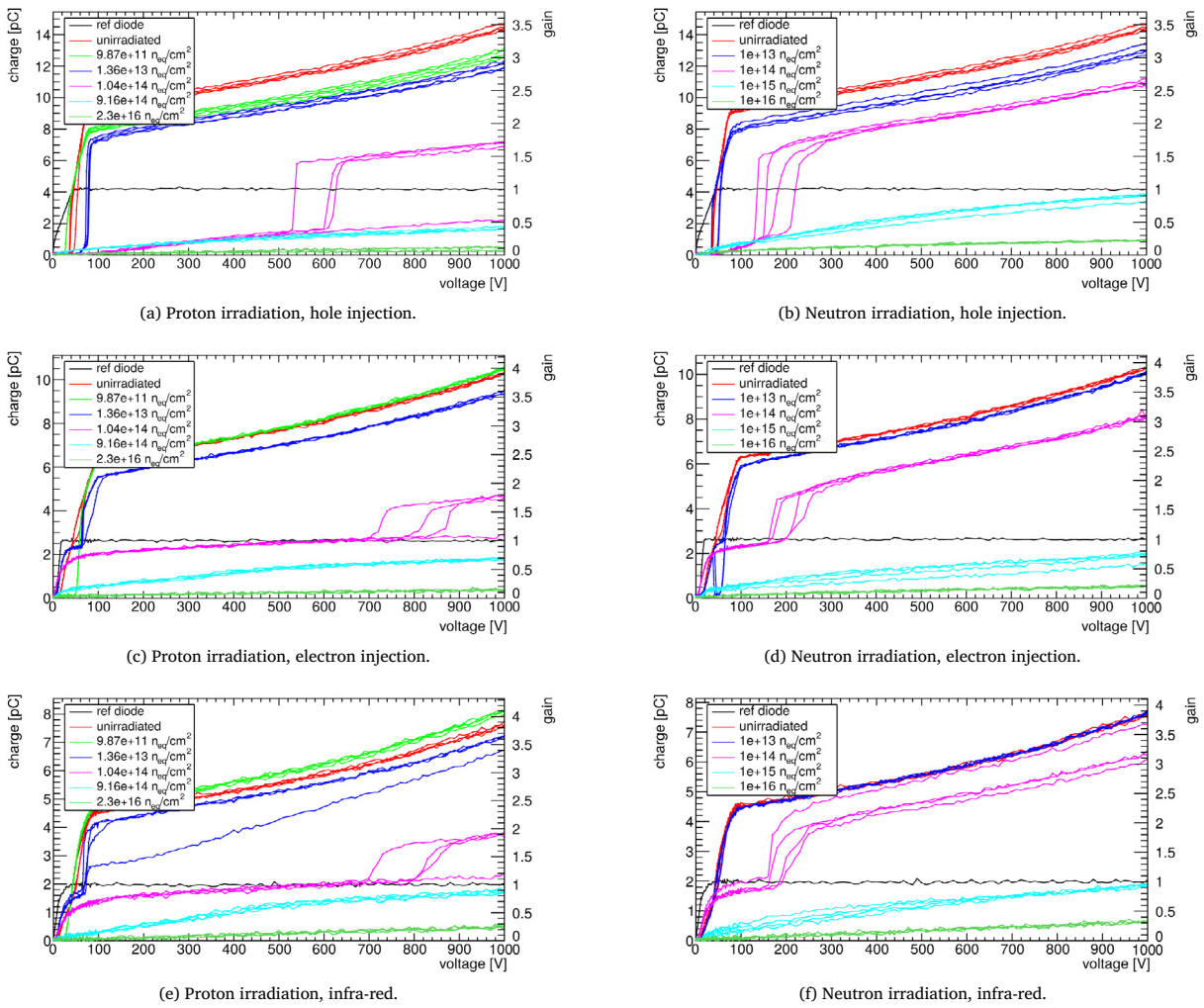

(a) Proton irradiation, hole injection.

(b) Neutron irradiation, hole injection.

(c) Proton irradiation, electron injection.

(d) Neutron irradiation, electron injection.

(e) Proton irradiation, infra-red.

(f) Neutron irradiation, infra-red.

Fig. 4. Charge collection and gain measurements for proton (left) and neutron (right) irradiated LGAD samples as a function of bias voltage at −20 °C. Each sample was measured at four different positions within the optical windows to investigate charge and gain variations. Hole injection (top), electron injection (center) and IR (bottom) TCT measurements have been performed on all samples and for all fluences. Due to the layout of the TCT system variations of the measurement positions between the hole and electron injection and IR pulses are possible. Measurements correspond to lot 7062.

Comparing the measured gain at a bias voltage of 1000 V as a function of fluence represented in Fig. 5 shows that the main gain decrease for both irradiation types takes place in the fluence range around 1×10^{14} n_{eq}/cm^2. For a bias voltage of 1000 V a gain of 1 is reached between 1×10^{14} n_{eq}/cm^2 and 1×10^{15} n_{eq}/cm^2. This means that the collected charge in a LGAD samples up to this fluence corresponds to a higher value than that in an unirradiated PIN diode. At fluences above 1×10^{15} n_{eq}/cm^2 the difference between the collected charge for electron and hole injection shown in Fig. 5(a) becomes less significant. This coincides with the fluence threshold at which charge multiplication cannot be observed any more. The results for IR pulses show a similar behavior for both types of irradiation. The only noticeable variation are the results for 1×10^{14} n_{eq}/cm^2 which show a gain difference between neutron and proton irradiation. This variation can be explained by a gradual acceptor removal which would indicate that proton irradiation seems to be more effective in removing acceptors than neutron irradiation if scaled to the same NIEL.

Gain measurement results with IR pulses and Sr90 source measurement at a bias voltage of 1000 V can be compared in Fig. 6. While the IR pulse measurements were performed with samples from lot 7062, the source measurements were performed on samples from lot 6474 [6] covering the fluence range from 1×10^{14} n_{eq}/cm^2 to 2×10^{15} n_{eq}/cm^2. The comparison of both lots and measurement techniques in Fig. 6 shows a good agreement in the tested fluence range. This comparison between source and TCT measurements is particularly interesting, as it demonstrates that TCT and source measurements give comparable absolute results for CCE data in highly irradiated silicon devices. An agreement that recently has also been reported in [20] and [19] where source and IR TCT measurements have been performed on highly irradiated (up to 10^{15} n_{eq}/cm^2) silicon diodes. No indication was found that ionization produced by beta particles and by IR light changes with particle fluence up to the fluence of about 10^{15} n_{eq}/cm^2, while there are expectations that the absorption behavior of IR light in irradiated silicon should change for higher fluences [21] and does become significant (> 5 % increase for 1060 nm) for fluences above 2×10^{15} n_{eq}/cm^2 [22].

The results in Fig. 6 also show an increased charge collection efficiency at the fluence of 1×10^{12} n_{eq}/cm^2 compared to the collected charge of an unirradiated LGAD sample which is used as a reference. The same effect is also visible as a function of voltage in Fig. 4.

3.3. Homogeneity study and TSC

Results presented in the previous chapter raised questions concerning the homogeneity of the layer and the corresponding charge amplification across the sensor surface. This becomes especially important for the application in high energy physics experiments which use the induced charge for their analysis or calibration. TCT measurements with electron and hole injection as shown in Fig. 3 were performed on three

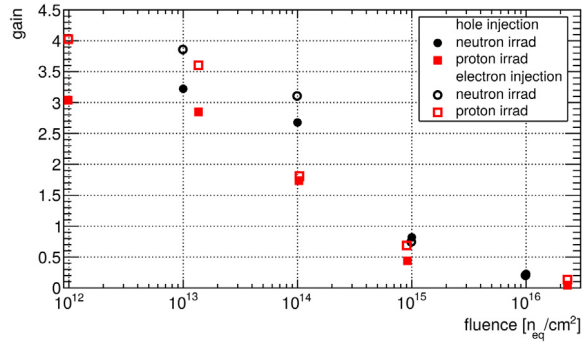

(a) Hole and electron injection.

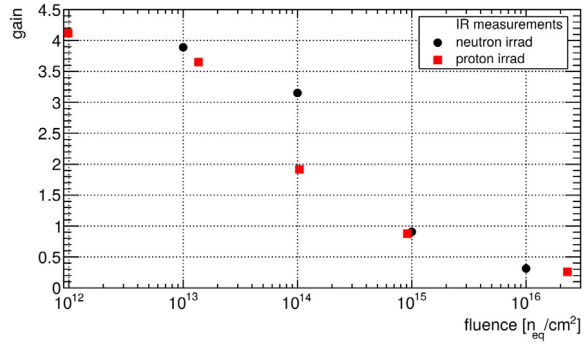

(b) IR pulses.

Fig. 5. Gain as a function of fluence based on hole and electron injection in Fig. 5(a) and IR pulses in Fig. 5(b) at a bias voltage of 1000 V for neutron and proton irradiated LGAD devices. The gain is defined as the ratio of the collected charge in a LGAD device to the collected charge of the undamaged reference sensor without amplification layer. Outliers shown in Fig. 4 were not considered for the analysis.

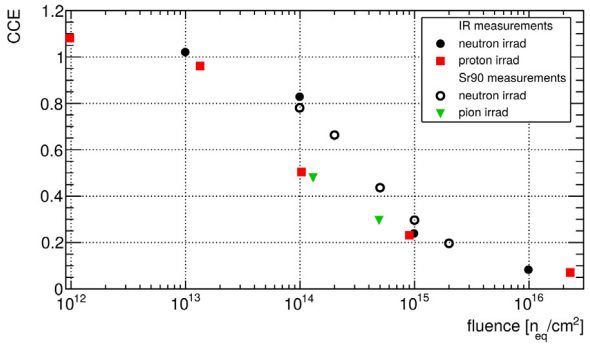

Fig. 6. Comparison of IR pulse measurements on samples from lot 7062 with source measurements using Sr90 of samples from lot 6474 at a bias voltage of 1000 V. The collected charge was scaled to 1 to ease the comparison. Source measurement results of lot 6474 were extracted of previous work [6].

unirradiated samples for bias voltages below and above full depletion. Apart from the charge loss regions observed for two samples in Fig. 3, homogeneous charge collection and gain were measured for voltages exceeding the full depletion voltage.

While uniform charge collection could be observed for high bias voltages, inhomogeneous charge collection regions appeared for voltages below full depletion. Electron injection measurements in Fig. 7 illustrate this effect for 50 V and 200 V. Similar results have also been observed for measurements with hole injection and IR pulses even showing the same pattern. A possible explanation that this behavior was not observed before is the preselection based on the leakage current

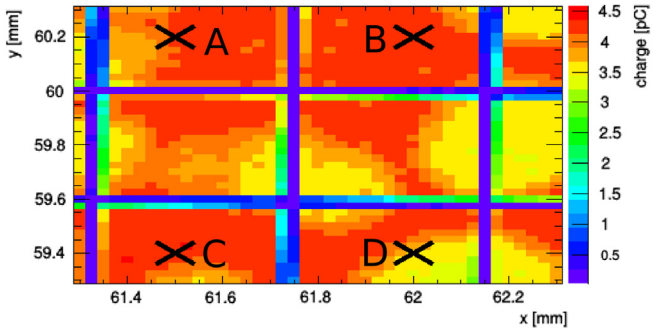

(a) 50 V.

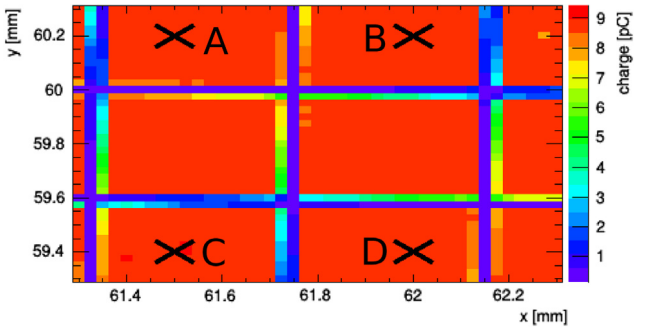

(b) 200 V.

Fig. 7. Surface scan with electron injection at 50 V (a) and 200 V (b) on an unirradiated device from lot 7062. In both cases the metal grid on the back side for the electrical contact becomes visible. The markers indicate four positions used to perform additional voltage scans with a higher voltage resolution. Additional scans have been performed with hole injection and IR pulses showing the same pattern at 50 V.

before irradiation [6]. While previous results were obtained for samples showing leakage current values below few μA, the leakage current of the samples in this study was above 40 μA. As devices with high and low leakage current were produced on the same wafer it was assumed that the implantation of the multiplication layer was not homogeneous over the entire wafer surface. These results led to additional measurements in order to determine the origin of the inhomogeneity.

Further investigating the signal shape within the inhomogeneous regions allows to determine unexpected features of the electric field. Waveforms in Fig. 8 taken at the positions indicated in Fig. 7 illustrate the electric field for bias voltages below and above full depletion. Electron injection signals corresponding to bias voltages above full depletion in Fig. 8(a) show the expected shape for electron and hole movement. The measurements A, B and C below full depletion in Fig. 8(b) also show the expected waveform for electron and hole movement. The waveform at position D on the other hand shows for the same conditions a signal corresponding to an inverted electric field indicated by the inverted gradient. In addition this inversion does not happen homogeneously but changes between the different positions and causes the variation in the charge collection across the surface. A similar behavior was also observed in earlier studies on irradiated LGAD samples [11]. TCT measurements based on electron injection performed on irradiated samples confirm these results. Waveforms at different bias voltages given in Fig. 9 for the 1×10^{14} n_{eq}/cm^2 neutron irradiated sample show a similar behavior as the unirradiated devices. For low bias voltages up to 200 V corresponds the signal shape to an inverted electric field. The signal shape for high bias voltages on the other hand shows the expected profile. The original explanation attributed the observed behavior to a modification of the space charge related to increased hole injection in the bulk after irradiation [6,11]. Since there are no hole traps expected in the material before irradiation it becomes difficult to

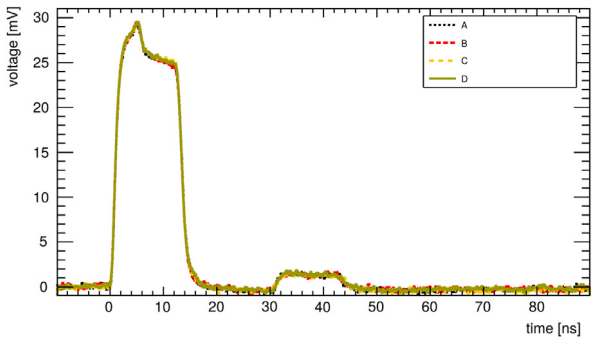

(a) 200 V - above full depletion voltage.

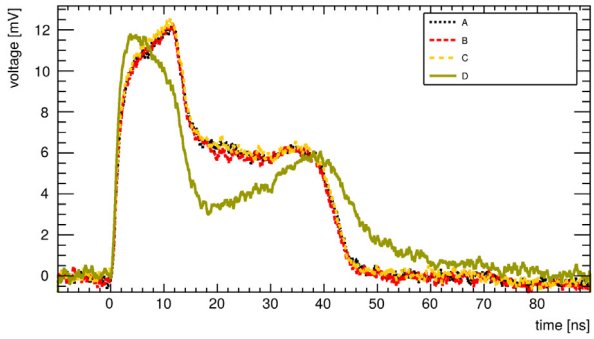

(b) 62 V - below full depletion voltage.

Fig. 8. Electron injection waveforms before irradiation corresponding to positions indicated in Fig. 7 for bias voltages below and above full depletion in (a) for 200 V and (b) for 62 V.

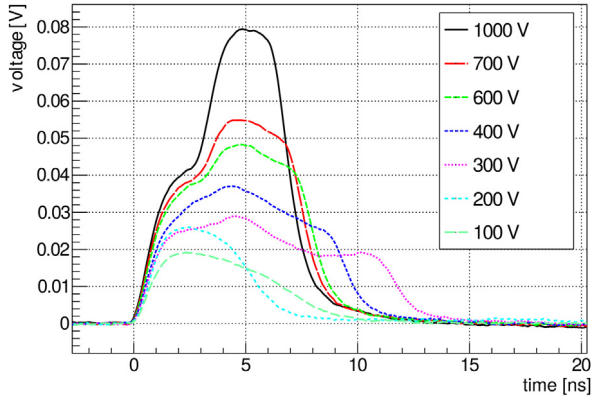

Fig. 9. Electron injection waveforms for the 1×10^{14} n_{eq}/cm^2 neutron irradiated sample for different bias voltages. Below 200 V signal shapes corresponding to an inverted electric field are visible which changes with increasing bias voltage.

explain this behavior for unirradiated samples. A possibility might be the deep implantation step during wafer treatment.

Comparing the gain obtained with TCT measurements of devices before irradiation with source measurements from a different lot using the same multiplication layer doping shows no variation for voltages above full depletion up to 1000 V [6,8]. This shows that the increased leakage current observed in the samples used in this study does not seem to impact on the gain performance above full depletion.

In irradiated devices no current and capacitance variations similar to unirradiated devices shown in Fig. 3 were observed. Since no measurements have been performed on these sensors before irradiation it remains unclear if the increased noise regions have been present in non-irradiated devices and disappeared after irradiation. Inhomogeneous

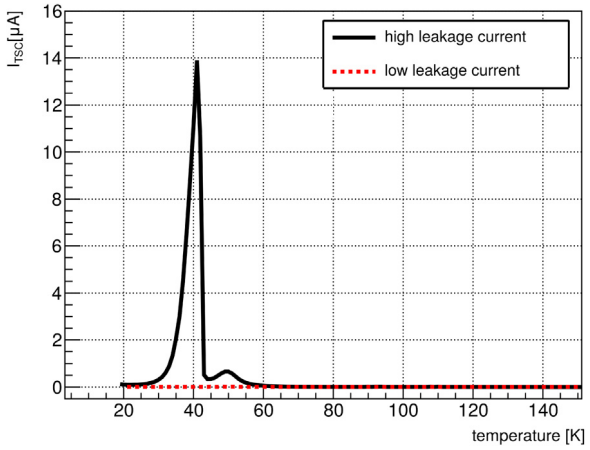

Fig. 10. Thermally stimulated current (TSC) measurement on unirradiated LGAD devices with high and low leakage current. The high leakage current device shows a peak in the TSC signal at 40 K.

charge collection regions on the other hand shifted as a function of fluence to higher bias voltages. To further investigate the inhomogeneous regions at low bias voltages which seem to be related to the inversion of the electric field, it was decided to perform thermally stimulated current (TSC) measurements on unirradiated devices with low and high leakage current. Unfortunately it was only possible to use samples from a second wafer of lot 7062 as no further unirradiated devices with low leakage current were available.

During the measurements the devices were biased at 100 V while the sample temperature was decreased to 20 K. Selecting a bias voltage above full depletion leads to empty charge traps when the minimum temperature is reached. In order to fill the charge traps a bias voltage is applied in forward direction. In this case a current limit of 1 mA was selected to avoid damaging the sensor. The filling step was applied for 200 s before the bias voltage was set again to 100 V. By increasing the temperature and measuring the leakage current, it becomes possible to determine the energy level of a charge trap. For this study the temperature of the device was increased by 10 K/min. Subtracting the leakage current in the unfilled state from the leakage current after filling allows to determine if a device contains defects and to draw conclusions about the type of defect.

The results in Fig. 10 show the measurements for samples with low and high leakage current. The one with low leakage current shows the expected low TSC signal which indicates that the device does not contain any defects. The sample with the high leakage current on the other hand shows a peak in the TSC signal at around 40 K. This behavior corresponds to charge traps in the silicon lattice which are not supposed to be present in unirradiated devices. As both samples were not irradiated a contamination of the wafer could be a possible reason for the increased leakage current. The observed defect level is too shallow to be responsible for the increased leakage current of the devices, but indicates that unwanted impurities or defects have been introduced into this specific production lot. The origin of the excess current in unirradiated devices remains unclear.

Preliminary tests have been performed on pad structures produced in the LGAD lot following lot 7062. Lot 7859 has been produced with a new mask file that implements pad structures with different sizes but also guard ring structures. The analysis of leakage current and TCT measurements performed on unirradiated samples from lot 7859 did not give any indication for inhomogeneous charge collection nor an excessively high leakage current. A set of 3 mm×3 mm samples was irradiated with protons in the CERN PS irradiation facility [23] and is available for the characterization with TCT and source measurements.

While the origin of the contamination in lot 7062 remains unclear, it can be assumed that a similar contamination is also the origin for the

increased leakage current behavior in lot 6474. For both lots samples with increased leakage current showed an unexpected bias dependent type inversion as well as a fluence dependent onset voltage for the amplification. As no gain variation could be observed for samples with low and high leakage current it can also be assumed that the contamination in samples with high leakage current does not affect the charge multiplication and with it the gain of the device.

4. Conclusion

Neutron and 800 MeV proton irradiated LGAD based silicon pad detectors with a multiplication layer dose of $1.6\times10^{13}\,cm^{-2}$ corresponding to a gain of about four have been investigated before and after irradiation. The focus was directed towards the intrinsic charge multiplication and gain of the devices based on TCT measurements with hole and electron injection as well as IR pulses. It was shown that the collected charge at a fluence in the order of $1\times10^{15}\,n_{eq}/cm^2$ corresponds to the charge of an unirradiated silicon PIN device. For higher fluences in the order of $1\times10^{16}\,n_{eq}/cm^2$ the gain corresponding to an unirradiated PIN device already fell below a value of 0.5. Comparing the results for neutron and proton irradiation but also with previous measurements in the fluence range below $1\times10^{15}\,n_{eq}/cm^2$ showed that the effective acceptor removal works faster for charged hadrons [6].

An increased leakage current observed in devices from two lots was investigated using the TSC method and was potentially attributed to a contamination in the silicon which led to inhomogeneous regions within a device. This contamination is also a possible origin of the type inversion and the amplification onset shift towards higher bias voltages observed in these devices. Nevertheless it remains necessary to investigate this behavior on irradiated LGAD structures of future lots. Preliminary measurements performed on a new LGAD processing lot performed at CNM including an enhanced pad structure design with a guard ring structure did not show an increased leakage current and no inhomogeneous regions within the device.

Acknowledgments

This work was developed in the framework of the CERN RD50 collaboration and partially financed by the Spanish Ministry of Economy, Industry and Competitiveness through the Particle Physics National Program (Ref. FPA2014-55295-C3-2-R and FPA2015-69260-C3-3-R) and co-financed with FEDER funds. We also want to thank the team of the CERN DSF bond lab, in particular Florentina Manolescu and Ian McGill for their help and support.

References

[1] Letter of Intent for the Phase-II Upgrade of the ATLAS Experiment, CERN, 2012. http://cds.cern.ch/record/1502664.

[2] D. Contardo, M. Klute, J. Mans, L. Silvestris, J. Butler, Technical Proposal for the Phase-II Upgrade of the CMS Detector, CERN, 2015. http://cds.cern.ch/record/2020886.

[3] H. F.-W. Sadrozinski, M. Baselga, S. Ely, V. Fadeyev, Z. Galloway, J. Ngo, C. Parker, D. Schumacher, A. Seiden, A. Zatserklyaniy, N. Cartiglia, G. Pellegrini, P. Fernández-Martínez, V. Greco, S. Hidalgo, D. Quirion, Sensors for ultra-fast silicon detectors, NIM A 765 (2014) 7–11. http://dx.doi.org/10.1016/j.nima.2014.05.006.

[4] N. Cartiglia, M. Baselga, G. Dellacasa, S. Ely, V. Fadeyev, Z. Galloway, S. Garbolino, F. Marchetto, S. Martoiu, G. Mazza, J. Ngo, M. Obertino, C. Parker, A. Rivetti, D. Shumacher, H F-W Sadrozinski, A. Seiden, A. Zatserklyaniy, Performance of ultra-fast silicon detectors, JINST 9 (02) (2014) C02001. http://stacks.iop.org/1748-0221/9/i=02/a=C02001.

[5] G. Pellegrini, P. Fernández-Martínez, M. Baselga, C. Fleta, D. Flores, V. Greco, S. Hidalgo, I. Mandić, G. Kramberger, D. Quirion, M. Ullan, Technology developments and first measurements of Low Gain Avalanche Detectors (LGAD) for high energy physics applications, NIM A 765 (2014) 12–16. http://dx.doi.org/10.1016/j.nima.2014.06.008.

[6] G. Kramberger, M. Baselga, V. Cindro, P. Fernández-Martínez, D. Flores, Z. Galloway, A. Gorišek, V. Greco, S. Hidalgo, V. Fadeyev, I. Mandić, M. Mikuž, D. Quirion, G. Pellegrini, H. F.-W. Sadrozinski, A. Studen, M. Zavrtanik, Radiation effects in Low Gain Avalanche Detectors after hadron irradiations, JINST 10 (07) (2015) P07006. http://stacks.iop.org/1748-0221/10/i=07/a=P07006.

[7] http://rd50.web.cern.ch/rd50/.

[8] V. Greco, P. Fernández-Martínez, D. Flores, S. Hidalgo, G. Pellegrini, D. Quirion, M. Baselga, N. Cartiglia, G. Kramberger, S. Grinstein, J. Lange, M. Fernández García, I. Vila, C. Gallrapp, M. Moll, V. Fadeyev, H. F.-W. Sadrozinski, R. Mori, U. Parzefall, R. Bates, G. Casse, Silicon Devices Optimised for Avalanche Multiplication, in: Proceedings, 23rd International Workshop on Vertex Detectors (Vertex 2014), PoS Vertex2014 (2015) 031. http://pos.sissa.it/archive/conferences/227/031/Vertex2014_031.pdf.

[9] Pablo Fernández-Martínez, D. Flores, S. Hidalgo, V. Greco, A. Merlos, G. Pellegrini, D. Quirion, Design and fabrication of an optimum peripheral region for low gain avalanche detectors, NIM A 821 (2016) 93–100. http://dx.doi.org/10.1016/j.nima.2016.03.049.

[10] G. Pellegrini, M. Baselga, M. Carulla, V. Fadeyev, P. Fernández-Martínez, M. Fernández García, D. Flores, Z. Galloway, C. Gallrapp, S. Hidalgo, Z. Liang, A. Merlos, M. Moll, D. Quirion, H. F.-W. Sadrozinski, M. Stricker, I. Vila, Recent technological developments on LGAD and iLGAD detectors for tracking and timing applications, NIM A 831 (2016) 24–28. http://dx.doi.org/10.1016/j.nima.2016.05.066.

[11] G. Kramberger, V. Cindro, I. Mandić, M. Mikuž, M. Zavrtanik, G. Pellegrini, M. Baselga, V. Greco, S. Hidalgo, P. Fernández-Martínez, D. Quirion, V. Fadeyev, H.F.-W. Sadrozinski, Effects of irradiation on LGAD devices 490 with high excess current, 25th RD50 Workshop (CERN) (2014) https://indico.cern.ch/event/334251/contributions/780778/.

[12] M. Ravnik, R. Jeraj, Research reactor benchmarks, Nucl. Sci. Eng. 145 (2003) 145–152.

[13] P.W. Lisowski, C.D. Bowman, G.J. Russell, S.A. Wender, The Los Alamos National laboratory spallation neutron sources, Nucl. Sci. Eng. 106 (1990) 208–218.

[14] P.W. Lisowski, K.F. Schoenberg, The Los Alamos neutron science center, NIMA 562 (2006) 910–914. http://dx.doi.org/10.1016/j.nima.2006.02.178.

[15] J. Becker, Signal Development in Silicon Sensors used for Radiation Detection, Universität Hamburg, 2010.

[16] M. Born, E. Wolf, Principles of Optics: Electromagnetic Theory of Propagation, Interference and Diffraction of Light, Cambridge University Press, 1999.

[17] R. Dalal, G. Jain, A. Bhardwaj, K. Ranjan, TCAD simulation of low gain avalanche detectors, NIMA 836 (2016) 113–121. http://dx.doi.org/10.1016/j.nima.2016.08.053.

[18] V. Eremin, N. Strokan, E. Verbitskaya, Z. Li, Development of transient current and charge techniques for the measurement of effective net concentration of ionized charges (Neff) in the space charge region of p-n junction detectors, NIMA 372 (1996) 388–398. http://dx.doi.org/10.1016/0168-9002(95)01295-8.

[19] E. Currás, M. Fernández García, C. Gallrapp, L. Gray, M. Mannelli, P. Meridiani, M. Moll, S. Nourbakhsh, C. Scharf, P. Silva, G. Steinbrueck, T. Tabarelli de Fatis, I. Vila, Radiation hardness and precision timing study of silicon detectors for the CMS High Granularity Calorimeter (HGC), NIMA 845 (2016) 60–63. http://dx.doi.org/10.1016/j.nima.2016.05.008.

[20] T. Pöhlsen, Charge Losses in Silicon Sensors and Electric-Field Studies at the Si-SiO2 Interface, Universität Hamburg, 2013.

[21] H.Y. Fan, A.K. Ramdas, Infrared absorption and photoconductivity in irradiated silicon, J. Appl. Phys. 30 (1959) 1127–1134. http://dx.doi.org/10.1063/1.1735282.

[22] Private communication with C. Scharf, Hamburg University; work presented on the DPG Frühjahrstagung, Germany, Hamburg, March 2016, Absorption of light, drift velocity, and trapping times in highly irradiated silicon pad sensors.

[23] F. Ravotti, B. Gkotse, M. Glaser, P. Lima, E. Matli, M. Moll, A new high-intensity proton irradiation facility at the CERN PS east area, in: Proceedings, 3rd International Conference on Technology and Instrumentation in Particle Physics (TIPP 2014), PoS TIPP2014 (2014) 354.